Phosphinic peptides, the first potent inhibitors of astacin, behave as extremely slow-binding inhibitors

Irene YIALLOUROS*[1], Stamatia VASSILIOU†, Athanasios YIOTAKIS†, Robert ZWILLING*, Walter STÖCKER*[1] and Vincent DIVE‡[2]

*Zoologisches Institut der Universität Heidelberg, Physiologie, Im Neuenheimer Feld 230, D-69120 Heidelberg, Germany, †Department of Organic Chemistry, Laboratory of Organic Chemistry, University of Athens, Panepistimiopolis, Zografou, Athens 15771, Greece, and ‡CEA, Département d'Ingénierie et d'Etudes des Protéines, C.E. Saclay, 91191 Gif/Yvette Cedex, France

A series of phosphinic pseudo-peptides varying in length and composition have been designed as inhibitors of the crayfish zinc endopeptidase astacin, the prototype of the astacin family and of the metzincin superfamily of metalloproteinases. The most efficient phosphinic peptide, fluorenylmethyloxycarbonyl-Pro-Lys-PheΨ(PO_2CH_2)Ala-Pro-Leu-Val, binds to astacin with a K_i value of 42 nM, which is about three orders of magnitude below the corresponding values for previously used hydroxamic acid derivatives. However, the rate constants for association (k_{on} = 96.8 $M^{-1} \cdot s^{-1}$) and dissociation ($k_{off} = 4.1 \times 10^{-6}$ s^{-1}) are evidence for the extremely slow binding behaviour of this compound. N-terminally or C-terminally truncated phosphinic analogues of this parent molecule are much less potent, indicating a critical role of the peptide size on the potency. In particular, omission of the N-terminal proline residue leads to a 40-fold increase in K_i which is mostly due to a 75-fold higher k_{off} value. These findings are consistent with the previously solved crystal structure of astacin complexed with one of the phosphinic peptides, benzyl-oxycarbonyl-Pro-Lys-PheΨ(PO_2CH_2)Ala-Pro-O-methyl, K_i = 14 μM [Grams, Dive, Yiotakis, Yiallouros, Vassiliou, Zwilling, Bode and Stöcker (1996) Nature Struct. Biol. **3**, 671–675]. This structure also reveals that the phosphinic group binds to the active site as a transition-state analogue. The extremely slow binding behaviour of the phosphinic peptides is discussed in the light of the conformational changes involving a unique 'tyrosine switch' in the structure of astacin upon inhibitor binding. The phosphinic peptides may provide a rational basis for the design of drugs directed towards other members of the astacin family which, like bone morphogenetic protein 1 (BMP1; i.e. the procollagen C-proteinase), have become targets of pharmacological research.

INTRODUCTION

Astacin, a zinc endopeptidase from the crayfish *Astacus astacus* L., is the prototype for the astacin family of zinc peptidases [1,2]. This protein family includes enzymes involved in peptide processing, like the cell surface peptidases meprin A and B of mammalian tissues [3,4], and also proteins playing critical roles in embryonic development and tissue differentiation, like bone morphogenetic protein 1 (BMP-1) found in diverse organisms [5–7]. Recently, the BMP-1 protein was reported to be identical with the procollagen C-proteinase, a zinc peptidase essential for the processing of procollagen during the assembly of fibrillar collagens [8–10].

Based on the structural topology of their catalytic modules, the astacins are grouped in the 'metzincin superfamily' together with the serralysins, the adamalysins/reprolysins and the matrix metalloproteinases (MMPs) [2,11]. While synthetic hydroxamate peptides proved to be potent inhibitors of MMPs [12], such types of compounds behave only as rather weak inhibitors of astacins [13,14], limiting their use both for exploring the basic functions of astacins and for pharmacological studies.

In an effort to obtain astacin inhibitors with higher binding affinity, the synthesis of phosphinic peptides has been undertaken [15–17]. The phosphinic group serves as a tetrahedral transition-state analogue, mimicking a water-attacked peptide bond of a substrate during hydrolysis. We were recently able to determine the structure of one of these transition-state analogues [Z-Pro-Lys-PheΨ(PO_2CH_2)Ala-Pro-OMe] bound to the active-site of astacin [18], where Z is benzyloxycarbonyl and OMe is the O-methyl group. In the present paper we report on the kinetics of the interaction of this phosphinic peptide, as well as those of other phosphinic analogues. These data and the potencies of these new inhibitors are discussed in view of the structural studies performed on astacin, which, as yet, is the only member of this protein family whose three-dimensional structure is known.

MATERIALS AND METHODS

Enzyme

The zinc endopeptidase astacin was purified from the digestive juice of the freshwater crayfish *A. astacus* L., as described previously (for refs. see [14]).

Inhibitor synthesis

Phosphinic peptides were synthesized by the solid-phase method, as described previously [19,20], using $Fmoc_{(L,D)}$PheΨ[PO(OAd)CH_2]$_{(L,D)}$AlaOH, $Fmoc_{(L,D)}$(boc)LysΨ[PO(OAd)CH_2]$_{(L,D)}$AlaOH or $Fmoc_{(L,D)}$PheΨ[PO(OAd)CH_2]GlyOH as building

Abbreviations used: BMP-1, bone morphogenetic protein 1; MMP, matrix metalloproteinase; Z, benzyloxycarbonyl; Fmoc, 9-fluorenylmethyloxycarbonyl; OMe, O-methyl; Ψ indicates replacement of the peptide bond by the group given in parentheses.

[1] Present address: Institut für Zoophysiologie, Molekulare Physiologie, Universität Münster, Hindenburgplatz 55, D-48143 Münster, Germany.
[2] To whom correspondence should be addressed (e-mail dive@dsvidf.cea.fr).

Table 1 Phosphinate inhibitors of astacin

The inhibition kinetics were conducted in 50 mM Hepes, pH 8, using the substrates Dns-PKRAPWV (**) or succinyl-Ala-Ala-Ala-4-nitroanilide (*), and 1×10^{-9} M or $5.0–5.5 \times 10^{-8}$ M enzyme respectively. P_1, P_2, P_3 and P_1', P_2', P_3' etc. denote the positions N- or C-terminal of the scissile bond ($\bigtriangledown$), where a corresponding peptide substrate would be cleaved respectively. PC, $\Psi(PO_2CH_2)$.

(a) Kinetic parameters

Peptide	k_{on} ($M^{-1} \cdot s^{-1}$)	$k_{off} \times 10^4$ (s^{-1})	k_i [μM]	$t_{\frac{1}{2}}$ ([I] = K_i)
P_4 ---P_3 P_2 P_1 $\bigtriangledown$ $P_1'P_2'P_3'P_4'$				
1. Z------P K F^{PC}A P------ OMe	–	–	10.0 (± 0.6)**	–
	14.3 (± 1.2)*	2.0 (± 0.8)*	14.0 (6.6)*	41.6 min
2. Z------P K F^{PC}A P L---- OMe	–	–	0.17 (0.01)**	–
	51.5 (± 0.7)*	0.13 (± 0.007)*	0.24 (± 0.01)*	11 h
3. Fmoc --P K F^{PC}A P L V- OH	–	–	0.036 (± 0.0007)**	–
	96.8 (± 2.7)*	0.041*	0.042*	34 h
4. Fmoc -------K F^{PC}A P L V- OH	–	–	3.7 (± 0.3)**	–
	167.9 (± 2.7)*	–3.1 (± 0.9)*	1.8 (± 32)*	–27 min
5. Fmoc ---------- F^{PC}A P L V- OH	–	–	3.6 (± 0.2)**	–
	163.5 (± 5.5)*	2.2 (± 0.5)*	1.3 (± 0.3)*	38 min
6. Z------ P K K^{PC}A P L V- OMe	344.0 (± 6.7)*	0.37*	0.11*	3.88 h
7. Z------ P K F^{PC}G P------ OMe	–	–	580.0 (± 4.3)**	–
8. Z------ P K F^{PC}G P L---- OMe	–	–	11.0 (± 0.2)**	–

(b) Assay conditions

Peptide	Succinyl-Ala-Ala-Ala-4-nitroanilide* (mM)	Dns-PKRAPWV** [mM]	Inhibitor (μM)	HPLC peak	Preincubation (h)
1. Z------P K F^{PC}A P------ OMe	2	0.1	0.12–100**	2	18**
			7.3–180*	–*	
2. Z------P K F^{PC}A P L---- OMe	0.6	0.1	0.005–100**	3	73**
			0.1–1.7*	–*	
3. Fmoc --P K F^{PC}A P L V- OH	0.6	0.1	0.05–4.6**	3	18**
			0.3–1*	–*	
4. Fmoc -------K F^{PC}A P L V- OH	2	0.05	0.001–100**	3	40**
			0.5–20*	–*	
5. Fmoc ---------- F^{PC}A P L V- OH	2	0.05	0.002–100**	1	41**
			0.8–20*	–*	
6. Z------ P K K^{PC}A P L V- OMe	0.6	–	0.02–1*	2	–*
7. Z------ P K F^{PC}G P------ OMe	–	0.1	0.094–190**	2	44**
8. Z------ P K F^{PC}G P L---- OMe	–	0.1	0.12–120**	2	41**

blocks during the peptide-chain elongation [21] (Fmoc is 9-fluorenylmethyloxycarbonyl; boc is t-butoxycarbonyl; OAd is *O*-adamantyl). The corresponding diastereomeric forms of these phosphinic peptides were purified and separated by preparative HPLC (Vydac 218TP1022 column), resulting in maximally four or two different peaks for each phosphinic peptide respectively. For each peptide, the potencies of the different diastereomers, present as separated HPLC peaks, were determined. Kinetic studies were performed only on the most active diastereomers, and their corresponding HPLC peaks are indicated in Table 1(b). In the cases of compounds 1 and 5, the most active HPLC peaks turned out to contain two diastereomers, which could not be resolved further by HPLC. Thus, for these compounds, the kinetic analysis was conducted with the mixture of two diastereomers. The composition of the phosphinic peptides was proved by MS.

Inhibition assays

Determination of k_{on} and k_{off} using progress-curve analysis

Progress curves were recorded at 25 °C in a thermostated spectrophotometer (UV/VIS Spectrometer Lambda 2S, Perkin-Elmer) by monitoring the release of 4-nitroaniline from the substrate succinyl-Ala-Ala-Ala-4-nitroanilide at 405 nm in 50 mM Hepes buffer, pH 8.0 [14]. Over a period of 2–44 h up to 9999 data points were recorded directly by means of the enzyme kinetics program PECSS (Perkin-Elmer).

In each case, the reaction was initiated by addition of enzyme into a cuvette containing a mixture of 0.6 mM substrate and varying inhibitor concentrations in 50 mM Hepes, pH 8.0. The pH value and the substrate concentration of the single reactions were measured at the end of the assay. The curves were fitted to eqn. (1) by non-linear least-squares analysis [22].

$$P = v_s t + (v_o - v_s)(1 - e^{-k_{app} t})/k_{app} \quad (1)$$

(P = product concentration, v_o = velocity at $t = 0$, v_s = steady-state velocity, k_{app} = observed first-order rate constant) using the program ENZFITTER (Elsevier–Biosoft, Cambridge, U.K.). If the plot of k_{app} versus the corresponding inhibitor concentrations [I] resulted in a straight line (see for example Figure 1b), then k_{on} and k_{off} were obtained according to eqn. (2)

$$k_{app} = k_{off} + k_{on}[I]/(1 + [S]/K_m) \quad (2)$$

The k_{off} values of the heptapeptides were estimated from the time course of enzyme–inhibitor (EI) complex dissociation. The complexes were prepared by incubation of equimolar amounts of enzyme and inhibitor (10^{-5} M) at 25 °C. Complex dissociation was achieved by diluting the EI complexes 100- to 1000-fold in a

cuvette containing succinyl-Ala-Ala-Ala-4-nitroanilide substrate in 50 mM Hepes, pH 8.0 [22–27]. After equilibrium was reached, the recorded time–response curves were fitted to eqn. (1). In this case, the k_{app} value obtained can be used as an approximation of k_{off}. For incomplete dissociation k_{off} is obtained from eqn. (3) [23,27]

$$[EI]/[EI]_o = e^{-k_{off} \times t} \quad (3)$$

The logarithmic plot of the enzyme activity $[\ln(v_s - v)/(v_s - v_z)]$ versus time results in a straight line, whose negative slope corresponds to $-k_{off}$; v_z is the initial rate and v is the rate at any time t of the reaction. The steady-state velocity (v_s) was then taken from separately measured references. k_{off} values for various EI concentrations were averaged. K_i values were calculated according to eqn. (4)

$$K_i = k_{off}/k_{on} \quad (4)$$

and the half-life $t_{\frac{1}{2}}$ for reaching equilibrium was calculated for $[I] = K_i$ using eqn. (5)

$$1/t_{\frac{1}{2}} = k_{off} + k_{on}[I]_o \quad (5)$$

Determination of K_i values at equilibrium

Increasing concentrations of inhibitor were incubated with a constant amount of enzyme at 25 °C until equilibrium was reached. The initial rates of the remaining free enzyme were measured after addition of a constant concentration of substrate. K_i values were determined by non-linear least-squares analysis (ENZFITTER, Elsevier–Biosoft, Cambridge, U.K.) using eqn. 6 [23,27]

$$v_i/v_o = \{1 - [(I_o + E_o + K_i) - (I_o + E_o + K_i)^2 - 4 \times E_o \times I_o]^{\frac{1}{2}}\}/2 \times E_o \quad (6)$$

The K_i values of the phosphinate inhibitors were determined fluorimetrically (Luminescence Spectrometer LS 50, Perkin-Elmer) using the dansylated substrate Dns-PKRAPWV [14,28]. The reaction mixture (400 μl) contained 1×10^{-9} M astacin, a fixed substrate concentration and variable inhibitor concentrations in 50 mM Hepes, pH 8 (concentrations are given in Table 1).

RESULTS AND DISCUSSION

The synthesis of phosphinic peptides, with sequences matching the specificity requirements of astacin, resulted in the characterization of the first potent inhibitors of this zinc protease. For comparison, the most efficient peptide hydroxamate inhibitors of astacin reported to date displayed a K_i value of 16 μM [13,14]. The data displayed in Table 1 demonstrate the importance of the size of the inhibitor for affinity. Whereas the phosphinic pentapeptide (compound 1) displays a K_i value of 14 μM, elongation of this inhibitor on its C-terminal side by one residue (compound 2) or two residues (compound 3) increases the affinity by factors of 100 and 500 respectively. Strikingly, the removal of the proline in the P_3 position (compound 3 compared with compound 4) results also in a 100-fold loss of potency. Regarding the role of the residues flanking the phosphinic bond, the data reveal that the substitution Phe → Lys in position P_1 of the inhibitor (3 compared with 6) has only a marginal effect on the affinity. In this case, a 10-fold decrease in the k_{off} value is counterbalanced by a 2-fold increase in the k_{on} value. In contrast, the substitution Ala → Gly in the P_1' position (1 compared with 7, and 2 compared with 8) promotes a 40–65-fold loss of potency.

In the absence of inhibitor, the steady-state rate of substrate hydrolysis by astacin is reached instantaneously and remains constant over the time scale monitored (Figure 1). In the presence of all phosphinic peptides used in this study, there is a time-dependent decrease in the steady-state rate as a function of the inhibitor concentration (Figure 1a). Even for the most potent inhibitor of this series (compound 3) at a concentration of 64 nM, the steady state is reached only after about 30 h (Figure 1a). From such progress curves, apparent first-order rate constants, k_{app}, were obtained and plotted versus the corresponding inhibitor concentrations. In the range of inhibitor concentrations used, these plots resulted in straight lines, which indicates that the binding of phosphinic transition-state analogues to astacin is a single-step rather than a two-step process. Hence, the data could be fitted to eqn. (2), from which the corresponding second-order association rate constants for different inhibitors were determined (Figure 1b and Table 1). The corresponding dissociation rate constants were obtained by recording the recovery of EI complex solutions, prepared as described in the Materials and methods section (Figure 1c). The k_{on} and k_{off} values reported in Table 1 indicate that the slow binding inhibition observed for these inhibitors is not only due to the low on-rate for EI formation, but results also from the very low degree of EI complex dissociation. Even for compound 1, a weak inhibitor, the k_{off} value corresponds to an average residence time of the inhibitor in the active site of the enzyme of 1 h. These kinetic data reveal also that the higher potency of compound 3, compared with the other inhibitors, is mainly the result of a decrease in the corresponding k_{off} values. Interestingly, while compounds 1 and 5 display almost the same k_{off} values, the former has a k_{on} value that is at least ten times lower than that measured for compound 5. Based on the structure of these two inhibitors, this observation implies that multiple interactions with the primed subsites in the active site of astacin might be more productive for faster association than interactions involving the non-primed subsites.

Previous studies on synthetic substrates of astacin have shown that optimal substrates contain at least seven residues [28], suggesting the importance of distal interactions for ensuring efficient binding and catalysis of the substrate. This has been corroborated by elucidation of the three-dimensional structure of astacin [29], which revealed a remarkably long active-site cleft. The data reported in the present study, showing a dramatic reduction of binding affinity with decreasing length of the phosphinic peptides, are in line with these observations. The structure of astacin in complex with compound 1 also reveals important features of the inhibitor interactions [18]. This inhibitor fits perfectly into the active-site cleft by aligning in an antiparallel manner to the edge β-strand of the upper subdomain of astacin. The five side-chains of the inhibitor are in close contact with the five defined subsites in the cleft [18]. The oxygens of the phosphinyl group interact with the zinc atom and also with the side-chains of Glu-93 and Tyr-149 [18], mimicking what could be the interaction of the hydrated tetrahedral intermediate formed during the catalysis of the peptide bond substrate. Altogether, these observations are in good agreement with the view that this inhibitor acts as a transition-state analogue, except for its weak affinity. This may be explained by the fact that the backbone of this inhibitor forms only two direct hydrogen bonds with the edge strand in the active site of astacin, which is in contrast with numerous examples of peptide inhibitors interacting with the active site of proteases [30]. In addition, several water molecules mediate the interaction between this inhibitor and the enzyme. The few hydrogen bonds, as well as the participation of several water molecules in the interaction, may explain the low potency of compound 1, despite the presence of multiple contacts between

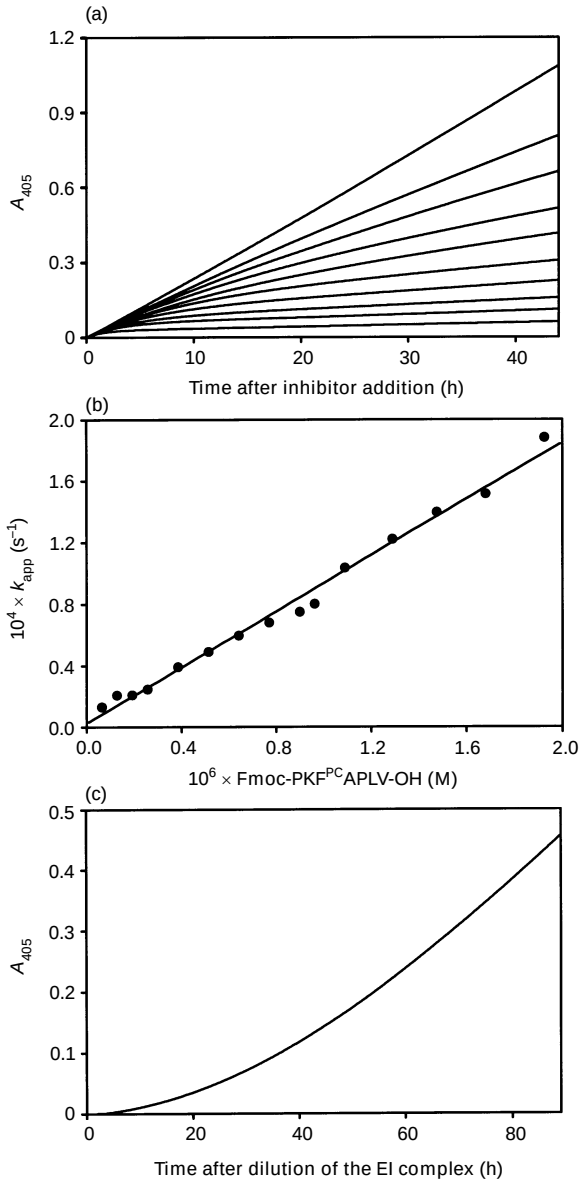

Figure 1 Binding of Fmoc-PKFΨ(PO_2CH_2)APLV-OH to astacin

(**a**) Time–response curve of the binding of the phosphinate inhibitor Fmoc-PKFΨ(PO_2CH_2)APLV-OH (64 nM to 1.9 μM) to astacin (52 nM), monitored in 50 mM Hepes, pH 8, with the substrate succinyl-Ala-Ala-Ala-4-nitroanilide (0.6 mM) at 405 nm. The curves correspond to inhibitor concentrations of (from the top) 0, 0.064, 0.13, 0.19, 0.26, 0.39, 0.51, 0.77, 1.1 and 1.9 μM respectively. From these curves k_{app}, the pseudo-first-order rate constant is obtained. (b) Plot of k_{app} versus inhibitor concentration. The slope of the straight line corresponds to the association rate constant $k_{on} = 96.8(\pm 2.7)\ M^{-1} \cdot s^{-1}$. (**c**) Dissociation of the complex of astacin with Fmoc-PKFΨ(PO_2CH_2)APLV-OH (0.029 μM) in 50 mM Hepes, pH 8. Recovered enzyme activity is monitored at 405 nm with the substrate succinyl-Ala-Ala-Ala-4-nitroanilide (0.34 mM). $k_{off} = 4.1 \times 10^{-6}\ s^{-1}$ is the average value from several curves with different initial concentrations.

the inhibitor and the enzyme [31,32]. Based on these observations, it might be hypothesized that the higher potency of compound 4 is due to the formation of additional hydrogen bonds in the EI complex, involving the C-terminal part of the inhibitor. Similarly, the 100-fold drop in the potency observed from compound 3 to 4 might suggest also a special role for the residue in the P_3 position of the inhibitor (Pro in compound 3), perhaps allowing the formation of optimal hydrogen-bond interactions between the lysine in the P_2 position and the active site of the protease [18]. Although substitutions of Pro in P_3 for Leu and Val in a series of substrates did not alter the substrate specificity dramatically [28], the appropriate occupation of the S_3 subsite of the enzyme by the P_3 residue of a phosphinic peptide inhibitor seems to be of principal importance.

However, apart from the above considerations, the structural analysis of the complex of astacin with compound 1, as compared with the structure of the free enzyme, has also revealed a number of conformational changes during complex formation [18]. The most intriguing one concerns the Tyr-149 switch, increasing the distance between the zinc and the phenolic oxygen from 2.5 Å to 5 Å, in the free and bound states respectively. The tyrosine switch is not mediated by $\chi 1$ or $\chi 2$ rotation of Tyr-149, but is mainly brought about by a rotation around the backbone. Simultaneously, the side-chain of Phe-154 gives way to the phenolic side-chain and the induced conformational change propagates along the C-terminal surface loops. In addition, an overall hinge movement of 1 Å is also observed, decreasing the distance between the rims of the lower and upper subdomains which define the active-site cleft. The conformational changes that occur along the pathway from the free to the bound state of astacin, as well as the formation of several hydrophobic contacts between the enzyme and the inhibitor, may also explain the particular kinetic behaviour of this inhibitor [33–35].

The astacin and serralysin families of zinc-peptidases are unique in having the zinc ion ligated by five residues, including a unique tyrosine [36–38]. Thus, if the tyrosine switch and the conformational changes following this movement is a conserved structural feature in these enzymes, it might be anticipated that transition-state analogue inhibitors of these proteases will also be slow binding. Studies of the interaction of similar phosphinic peptides with other members of the astacin or serralysin family appear consequently as an important issue to confirm the kinetic behaviour and the potency of such inhibitors. Compound 3, as the first potent inhibitor reported to date for astacin, may serve as a lead compound for the development of inhibitors directed against other members of the astacin family, such as meprin or the BMP-1 protease, a major target for blocking fibrosis [8]. Also, the screening of phosphinic peptide libraries [19,20] may represent a more systematic approach to identify potent inhibitors of this family of enzymes, as well as to detect faster binding inhibitors.

We thank Monika Dörhöfer (Heidelberg) for the preparation of astacin. This work was supported by the Deutsche Forschungsgemeinschaft (Sto 185/3-2).

REFERENCES

1 Stöcker, W., Gomis-Rüth, F. X., Bode, W. and Zwilling, R. (1993) Eur. J. Biochem. **214**, 215–231
2 Stöcker, W., Grams, F., Baumann, U., Reinemer, P., Gomis-Rüth, F.-X., McKay, D. B. and Bode, W. (1995) Protein Sci. **4**, 823–840
3 Dumermuth, E., Sterchi, E., Jiang, W., Wolz, R. L. and Bond, J. S. (1991) J. Biol. Chem. **266**, 21381–21385
4 Bond, J. S. and Beynon, R. B. (1995) Protein Sci. **4**, 1245–1261
5 Wozney, J. M., Rosen, V., Celeste, A. J., Mitsock, L. M., Whitters, M. J., Kriz, R. M., Hewick, R. H. and Wang, E. A. (1988) Science **242**, 1528–1534
6 Maéno, M., Xue, Y., Wodd, T. I., Ong, R. C. and Kung, H. (1993) Gene **134**, 257–261
7 Fukagawa, M., Suzuki, N., Hogan, B. L. M. and Jones, C. M. (1994) Dev. Biol. **163**, 175–183
8 Kessler, E., Takahara, K., Biniaminov, L., Brusel, M. and Greespan, D. S. (1996) Science **271**, 360–362
9 Li, S. W., Sieron, A. L., Fertala, A., Hojma, Y., Arnold, W. V. and Prockop, D. (1996) Proc. Natl. Acad. Sci. U.S.A. **93**, 5127–5130

10 Suzuki, N., Labosky, P. A., Furuta, Y., Hargett, L., Dunn, R., Fogo, A. B., Takahara, K., Peters, D. M. P., Greenspan, D. S. and Hogan, B. L. M. (1996) Development **122**, 3587–3595.
11 Bode, W., Gomis-Rüth, F.-X. and Stöcker, W. (1993) FEBS Lett. **331**, 134–140
12 Beckett, R. P., Davidson, A. H., Drummond, A. H., Huxley, P. and Whitaker, M. (1996) Drug Discovery Today **1**, 16–26
13 Wolz, R. L. (1994) Arch. Biochem. Biophys. **281**, 275–281
14 Stöcker, W. and Zwilling, R. (1995) Methods Enzymol. **248**, 305–325
15 Grobelny, D., Goli, U. and Galardy, R. E. (1989) Biochemistry **28**, 4948–4951
16 Morgan, B. P., Scholtz, J. M., Ballinger, M. D., Zipkin, I. D. and Bartlett, P. A. (1991) J. Am. Chem. Soc. **113**, 297–307
17 Yiotakis, A. Lecoq, A., Nicolaou, A. Labadie, J. and Dive, V. (1994) Biochem. J. **303**, 323–327
18 Grams, F., Dive, V., Yiotakis, A., Yiallouros, I., Vassiliou, S., Zwilling, R., Bode, W. and Stöcker, W. (1996) Nature Struct. Biol. **3**, 671–675
19 Jiracek, J., Yiotakis, A., Vincent, B., Lecoq, A., Nicolaou, A., Checler, F. and Dive, V. (1995) J. Biol. Chem. **270**, 21701–21706
20 Jiracek, J., Yiotakis, A., Vincent, B., Checler, F. and Dive, V. (1996) J. Biol. Chem. **271**, 19606–19611
21 Yiotakis, A., Vassiliou, S., Jiracek, J. and Dive, V. (1996) J. Org. Chem. **61**, 6601–6605
22 Cha, S. (1975) Biochem. Pharmacol. **24**, 2177–2185
23 Bieth, J. G. (1984) Biochem. Med. **32**, 387–397
24 Schloss, J. V. and Cleland, W. W. (1982) Biochemistry **21**, 4420–4427
25 Morrison, J. F. (1982) Trends Biochem. Sci. **7**, 102–105
26 Wilkes, B. H. and Prescott, J. M. (1985) J. Biol. Chem. **260**, 13154–13162
27 Bieth, J. G. (1995) Methods Enzymol. **248**, 59–84
28 Stöcker, W., Ng, M. and Auld, D. S. (1990) Biochemistry **29**, 10418–10425
29 Bode, W., Gomis-Rüth, F.-X., Huber, R., Zwilling, R. and Stöcker, W. (1992) Nature (London) **358**, 164–167
30 Rich, D. H. (1990) in Comprehensive Medicinal Chemistry, vol. 2 (Hansch, C., ed.), pp. 391–441, Pergamon Press, New York
31 Ringe, D. (1995) Curr. Opin. Struct. Biol. **5**, 825–829
32 Ladbury, J. E. (1996) Chem. Biol. **3**, 973–980
33 Brady, K., Wei, A., Ringe, D. and Abeles, R. H. (1990) Biochemistry **29**, 7600–7607
34 Bartlett, P. A. and Marlow, C. K. (1987) Biochemistry **26**, 8553–8561
35 Wolfenden, R. and Radzicka, A. (1991) Curr. Opin. Struct. Biol. **1**, 780–787
36 Gomis-Rüth, F.-X., Stöcker, W., Huber, R., Zwilling, R. and Bode, W. (1993) J. Mol. Biol. **229**, 945–968
37 Baumann, U., Bauer, M., Letoffé, S., Delepelaire, P. and Wandersman, C. J. (1995) J. Mol. Biol. **248**, 653–661
38 Baumann, U., Wu, S., Flaherty, K. M. and McKay, D. B. (1995) EMBO J. **12**, 3357–3364

Received 22 September 1997/2 February 1998; accepted 3 February 1998